

**CHIRAL PERTURBATION THEORY AND VECTOR MESONS**

**IN  $e^+e^- \rightarrow \pi^0\gamma$  AND  $\pi^0l^+l^-$ .**

A. Bramon

Grup de Física Teòrica, Universitat Autònoma de Barcelona,  
08193 Bellaterra (Barcelona), Spain

and

A. Grau and G. Pancheri

INFN, Laboratori Nazionali di Frascati,  
P.O.Box 13, 00044 Frascati, Italy

**Abstract**

The low-energy cross-section for  $e^+e^- \rightarrow \pi^0\gamma$  is predicted in ChPT at next-to-leading order and the saturation of its counter-terms by vector-meson resonances is confirmed. Further details on this saturation by vector-mesons are discussed for  $e^+e^- \rightarrow \pi^0\mu^+\mu^-$ . Cross-sections are predicted from threshold up to the  $\omega$ -mass region for different choices of the relevant parameters in the Lagrangian. It is suggested that measurements of these cross-sections at low-energy high luminosity  $e^+e^-$  machines, like Daphne, will allow to distinguish between different sets of parameters.

High luminosity  $\phi$  factories are expected to provide accurate data for reactions such as  $e^+e^- \rightarrow \pi^0\gamma$ ,  $\pi^0\gamma^*$ ,  $\pi^+\pi^-\pi^0\dots$  in the low energy region [1]. In this region, where perturbative QCD cannot be applied, Chiral Perturbation Theory (ChPT) has already shown its reliability and accuracy incorporating the low-energy theorems and providing their next-order corrections. The ChPT lagrangian contains an anomalous and a non-anomalous part. The latter begins with a fixed lowest order term,  $L_2$ , (order two in particle four-momenta or masses), followed by a series of higher-order counter-terms required to cancel the divergences originated in loop integrations. This part of the theory has been extensively studied (up to order four) by Gasser and Leutwyler [2], who fixed the values of the finite part of those counter-terms from experimental information. The possibility that these counter-terms could be dominated by the exchange of the known low-energy resonances has been investigated and fully confirmed by several authors [3], [4]. Concerning the anomalous part of the ChPT lagrangian, its lowest order term (order four) is given by the well-known Wess-Zumino lagrangian,  $L_{WZ}$  [5]. Next-order corrections have been studied by several authors [6, 7] but the situation is less satisfactory than in the non-anomalous case. We discuss the processes  $e^+e^- \rightarrow \pi^0\gamma$  and  $e^+e^- \rightarrow \pi^0\gamma^* \rightarrow \pi^0l^+l^-$  in an attempt to improve our knowledge on the anomalous sector.

The relevant part of the lowest-order anomalous lagrangian is

$$L_{WZ} = -i\frac{e^2}{8\pi^2}\epsilon^{\mu\nu\alpha\beta}\partial_\mu A_\nu A_\alpha \text{tr}[(Q^2 + \frac{1}{2}Q\Sigma Q\Sigma^\dagger)\partial_\beta\Sigma\Sigma^\dagger - (Q^2 + \frac{1}{2}Q\Sigma^\dagger Q\Sigma)\partial_\beta\Sigma^\dagger\Sigma] \\ - \frac{e}{16\pi^2}\epsilon^{\mu\nu\alpha\beta}A_\mu \text{tr}[Q(\partial_\nu\Sigma\partial_\alpha\Sigma^\dagger\partial_\beta\Sigma\Sigma^\dagger - \partial_\nu\Sigma^\dagger\partial_\alpha\Sigma\partial_\beta\Sigma^\dagger\Sigma)] + \dots \quad (1)$$

where the dots refer to non-photonic terms, irrelevant for our present purposes, and  $Q$  is the quark charge matrix  $Q=\text{diag}(2/3, -1/3, -1/3)$ . The octet of pseudoscalar mesons  $P \equiv \frac{1}{\sqrt{2}}\sum_i\lambda_i P_i$ , where  $\lambda_i$  are the eight Gell-Mann matrices with  $\text{tr}\lambda_i^2 = 2$ , appears in

$$\Sigma \equiv \Sigma_8 \equiv \exp[(2i/f)P], \quad (2)$$

which transforms as  $\Sigma \rightarrow U_L\Sigma U_R^\dagger$  under  $SU(3)_L \times SU(3)_R$  transformations. The constant  $f$  in (2) can be fixed from the charged pion decay width [8] leading to

$$f = 132 \text{ MeV} \quad (3)$$

From the first term in (1) one immediately deduces the amplitude for the  $\pi^0 \rightarrow \gamma\gamma$  decay,

$$A(\pi^0 \rightarrow \gamma\gamma) = i\frac{\alpha\sqrt{2}}{\pi f}\epsilon^{\mu\nu\alpha\beta}\epsilon_\mu k_\nu \epsilon'_\alpha k'_\beta, \quad (4)$$

which predicts  $\Gamma(\pi^0 \rightarrow \gamma\gamma) = \alpha^2 m_{\pi^0}^3 / (32\pi^3 f^2) = 7.6 \text{ eV}$  in good agreement with the experimental datum [8]  $\Gamma(\pi^0 \rightarrow \gamma\gamma) = 7.7 \pm 0.6 \text{ eV}$ .

The non-renormalization of the above (lowest order) result no longer holds when dealing with off-mass-shell photon(s), as in the  $\gamma\gamma^* \rightarrow \pi^0$  production amplitude. In

this case, one can write

$$A(\gamma\gamma^* \rightarrow \pi^0) = i \frac{\alpha\sqrt{2}}{\pi f} \epsilon^{\mu\nu\alpha\beta} \epsilon_\mu k_\nu \epsilon_\alpha^* k_\beta^* \left[ 1 + C_l(\mu, k^2) + C^r(\mu)k^2 \right], \quad (5)$$

where, apart from the lowest-order term (4), one has the corrections coming from loops and counterterms. The latter are necessary in order to cancel the divergences originated in loop integrations. The remaining finite parts of the loop and counterterm corrections depend on the renormalization mass scale  $\mu$ . This will be fixed around the  $\rho$ - and  $\omega$ -meson masses,  $\mu^2 \simeq m_{\rho,\omega}^2 \equiv (m_\rho^2 + m_\omega^2)/2 \simeq 0.60 \text{ GeV}^2$ , which are the relevant ones in our case. The correction due to pion and kaon loops is found to have a finite part given by [7]

$$C_l(\mu, k^2) = \frac{1}{48\pi^2 f^2} \left[ k^2 \log \frac{\mu^4}{m_\pi^2 m_K^2} + \frac{10}{3} k^2 + 4 F(m_\pi^2, k^2) + 4 F(m_K^2, k^2) \right] \quad (6)$$

with

$$F(m^2, k^2) = m^2 \left( 1 - \frac{x}{4} \right) \sqrt{\frac{x-4}{x}} \ln \frac{\sqrt{x} + \sqrt{x-4}}{-\sqrt{x} + \sqrt{x-4}} - 2m^2, \quad \text{for } x = \frac{k^2}{m^2} > 4$$

$$F(m^2, k^2) = 2m^2 \left( 1 - \frac{x}{4} \right) \sqrt{\frac{4-x}{x}} \arctg \sqrt{\frac{x}{4-x}} - 2m^2, \quad \text{for } x \leq 4$$

$$F(m^2, k^2) = -\frac{2k^2}{3} \quad \text{for } k^2 \ll m^2 \quad (7)$$

Then eq.(6) for  $k^2 \ll m_{\pi,K}^2$  reduces to

$$C_l(\mu, k^2) \simeq \frac{1}{48\pi^2 f^2} \left( \log \frac{\mu^4}{m_\pi^2 m_K^2} - 2 \right) k^2 \equiv k^2 / \Lambda_l^2, \quad \text{with } \Lambda_l^{-2} \simeq 0.28 \text{ GeV}^{-2}. \quad (8)$$

The relevant counterterm in the (order six) lagrangian is [7]

$$L_6 = i\epsilon^{\mu\nu\alpha\beta} F_{\alpha\beta} \partial^\lambda F_{\lambda\nu} \left\{ B_1 \text{tr}(Q^2 \Sigma^\dagger \partial_\mu \Sigma - Q^2 \Sigma \partial_\mu \Sigma^\dagger) + B_2 \text{tr}(Q \Sigma^\dagger Q \partial_\mu \Sigma - Q \Sigma Q \partial_\mu \Sigma^\dagger) \right\} \quad (9)$$

and implies

$$C^r(\mu) = -\frac{4\pi}{3\alpha} (B_1 + B_2) \quad (10)$$

The numerical value of (10) can be fixed from (up to now inconclusive) experiments on  $\pi^0 \rightarrow \gamma e^+ e^-$  decays [8] or from a recent experiment on  $\gamma^* \gamma \rightarrow \pi^0$  production through one (essentially) real photon and a virtual one [9]. The measured

$k^2$ -dependence of the amplitude can be linearly parametrized in terms of a slope parameter  $b_{\pi^0}$  as in eq.(5). Using also (8) and (10) one has [9]

$$b_{\pi^0}(exp) = (1.79 \pm 0.14) \text{ GeV}^{-2} = \frac{1}{\Lambda_l^2} - \frac{4\pi}{3\alpha}(B_1 + B_2) \quad (11)$$

and

$$B_1 + B_2 = -(1.13 \pm 0.11) \frac{\alpha}{\pi} \text{ GeV}^{-2} = -(0.68 \pm 0.07) \frac{\alpha}{\pi m_{\rho,\omega}^2} \quad (12)$$

This experimental result and its parametrization in terms of  $B_1 + B_2$  allows for a new test on the hypothesis of the saturation of the counterterms by resonance exchange. The non-strange  $\rho$  and  $\omega$  vector mesons are the relevant ones in our  $\gamma\gamma^*\pi^0$  coupling, as already mentioned when fixing  $\mu$  around  $m_{\rho,\omega}$ . The whole (ideally mixed) nonet of vector mesons,  $V$ , can easily be introduced in our approach as gauge bosons of a "hidden" local symmetry following the work of Bando and collaborators [10]. This procedure and the corresponding lagrangian can be found in refs.[7, 11]. Here we simply quote the pieces of the whole lagrangian (including also the first term from  $L_{WZ}$  (1)) dealing with  $P\gamma\gamma$ ,  $VP\gamma$  and  $VVP$  vertices, namely,

$$\begin{aligned} L_{P\gamma\gamma} &= \left( \frac{3}{4\pi^2} + 8a_3 \right) \frac{e^2}{f} \epsilon^{\mu\nu\alpha\beta} \partial_\mu A_\nu \partial_\alpha A_\beta \text{tr}(Q^2 P) \\ L_{VP\gamma} &= (a_2 - 2a_3) \frac{2eg}{f} \epsilon^{\mu\nu\alpha\beta} \partial_\mu A_\nu \text{tr}(Q(\partial_\alpha V_\beta P + P\partial_\alpha V_\beta)) \\ L_{VVP} &= -4a_2 \frac{g^2}{f} \epsilon^{\mu\nu\alpha\beta} \text{tr}(\partial_\mu V_\nu \partial_\alpha V_\beta P), \end{aligned} \quad (13)$$

where  $V$  is the vector meson  $SU(3)$  matrix [ with diagonal terms given by  $(\rho^0 + \omega)/\sqrt{2}$ ,  $(-\rho^0 + \omega)/\sqrt{2}$  and  $\varphi$ , due to  $\omega$ - $\varphi$  ideal mixing]. The constant  $g$  in (13) appears also in the lagrangian

$$L_{V\gamma} = f^2 \text{tr}(g^2 V_\mu V^\mu - 2eg Q A_\mu V^\mu + \dots) \quad (14)$$

containing, among other irrelevant terms, the vector meson mass-term with

$$g = m_{\rho,\omega}/\sqrt{2}f \simeq 4.15 \quad (15)$$

and the standard  $V\gamma$  couplings  $em_V^2/f_V$  with  $f_\rho = \frac{1}{3}f_\omega = \sqrt{2}g$ .

The  $\pi^0\gamma\gamma$  amplitude for real photons is given by eq.(4) and proceeds exclusively from the first term in  $L_{P\gamma\gamma}$ , eq. (13), (*i.e.*, the first term in  $L_{WZ}$ , eq.(1)), due to the cancellation of all  $a_{2,3}$  dependent terms once the  $V\gamma$  transition (14) is used. The  $a_{2,3}$  dependence appears when dealing with vertices such as  $\omega\pi^0\gamma$  or  $\pi^0\gamma\gamma^*$ , where

the virtual photon introduces also a  $k^{*2}$ -dependence through the vector meson form-factor  $m_{\omega,\rho}^2/(m_{\omega,\rho}^2 - k^{*2}) = 1 + k^{*2}/m_{\omega,\rho}^2 + \dots$ . Retaining up to the second term in this expansion allows for an identification of the  $B_{1,2}$  coefficients in  $L_6$ , eq.(9), in terms of  $a_{2,3}$  and their numerical values deduced from the datum  $\Gamma(\omega \rightarrow \pi^0\gamma) = (720 \pm 50)$  keV  $\simeq 9 \Gamma(\rho \rightarrow \pi\gamma)$  [8]. As shown in [7], one easily obtains

$$|B_1^V + B_2^V| = 2\pi^2 |a_2 + 2a_3| \frac{\alpha}{\pi m_{\rho,\omega}^2} = (0.73 \pm 0.02) \frac{\alpha}{\pi m_{\rho,\omega}^2} \quad (16)$$

in good agreement with (12), thus confirming the resonance saturation hypothesis for the counterterms,  $B_1 + B_2 \simeq B_1^V + B_2^V$ .

Apparently, this seems to indicate an equivalence between the model of Bando et al.[10], eqs.(13)and (14), and conventional vector-meson dominance (VMD) in this type of processes. Indeed, if one chooses

$$a_2 = 2a_3 = -3/16\pi^2, \quad a_2 + 2a_3 = -3/8\pi^2, \quad (17)$$

the lagrangian (13) contains no direct  $P\gamma\gamma$  and  $VP\gamma$  vertices [which are then exclusively generated by the  $L_{VVP}$  term and  $V\gamma$  conversion(s) from  $L_{V\gamma}$ , eq.(14)] as in conventional VMD. However, the agreement between eqs.(12) and (16) requires only  $a_2 + 2a_3 = -3/8\pi^2$ , fully compatible with the VMD value (17), but allowing for deviations from conventional VMD through  $a_2 \neq 2a_3$ . The possibility of these deviations has already been discussed in the related context of  $\gamma^* \rightarrow PPP$  transitions [11]. Moreover, data on the  $k^{*2}$ -dependence for the decay  $\omega \rightarrow \pi^0\gamma^* \rightarrow \pi^0\mu^+\mu^-$  [12] seem to require already  $a_2 \neq 2a_3$  in our present context. These data have been parametrized in terms of the usual e.m. transition form-factor  $F_\omega \equiv \Lambda^2/(\Lambda^2 - k^{*2})$  and imply  $\Lambda_{exp} = 0.65 \pm 0.03$  GeV, well below the expected  $\rho$ -meson mass  $m_\rho = 0.768$  GeV. This can easily be explained in terms of the lagrangians (13) and (14), which imply a form-factor given by  $1 + \frac{2a_2}{(a_2+2a_3)} \frac{k^{*2}}{m_\rho^2} + \dots$ , leading to  $a_2 = 4.6 a_3$  when compared (up to this order) to  $1 + \frac{k^{*2}}{\Lambda_{exp}^2} + \dots$ . For higher values of  $k^{*2}$  the data [12] tend to prefer values of  $a_2$  somewhat larger than  $5a_3$ ; so we will adopt

$$a_2 = 6a_3 = -9/32\pi^2, \quad a_2 + 2a_3 = -3/8\pi^2 \quad (18)$$

as a compromise which represents an interesting alternative to the VMD values (17). Apart from giving a reasonable description of the  $\omega \rightarrow \pi^0\mu^+\mu^-$  data, the values (18) are also in the preferred region (see ref.[11]) in order to account for the data on the  $\omega \rightarrow \pi^+\pi^-\pi^0$  width and the  $e^+e^- \rightarrow \pi^+\pi^-\pi^0$  cross-section. Moreover, recent analyses of the  $\omega \rightarrow \pi^0\mu^+\mu^-$  form-factor in the lattice seem to confirm [13] a clear deviation from conventional VMD. For all these reasons, we proceed to discuss the reactions  $e^+e^- \rightarrow \pi^0\gamma$  and  $e^+e^- \rightarrow \pi^0l^+l^-$ , which will clarify the whole situation and contribute to fix the value of the ChPT counterterms or the  $a_{2,3}$  parameters.

The  $e^+e^- \rightarrow \pi^0\gamma$  cross section at lowest order is given by  $L_{WZ}$  in eq.(1) and turns out to be

$$\sigma_{e^+e^- \rightarrow \pi^0\gamma}^{l.o.}(s) = \frac{\alpha^3}{12\pi^2 f^2} (1 - m_{\pi^0}^2/s)^3, \quad (19)$$

where  $s$  is the square of the total CM energy and  $\alpha^3/(12\pi^2 f^2) = 0.0734$  nb. This lowest order cross section (19) is shown (dotted line) in Fig.1. Next order corrections in ChPT include the effects of loops and counterterms as in eq.(5). For the latter, the resonance saturation assumption implies  $C^r(\mu \simeq m_{\rho,\omega}) = 1/m_{\rho,\omega}^2$ , as follows from (10),(16), and (17) or (18), thus increasing the lowest order amplitude up to a 60% at  $E = \sqrt{s} = 0.6$  GeV as also shown (dashed line) in Fig.1. The associated loop corrections are given by  $C_l(\mu, s)$  in eq.(6). These loop corrections are considerably smaller than those coming from the corresponding counterterms (around a 15% in the amplitude) and slightly increase the  $e^+e^- \rightarrow \pi^0\gamma$  cross-section, as shown (dot-dashed line) in Fig.1. This curve represents the full ChPT prediction at next-to-leading order for  $e^+e^- \rightarrow \pi^0\gamma$  and is expected to reproduce future data in the low energy region.

Around the resonance masses the cross-section is quite different as indicated by the datum (shown with error bars in Fig.1)  $\sigma_{e^+e^- \rightarrow \pi^0\gamma}(s = m_\omega^2) = 152 \pm 13$  nb at the  $\omega$ -peak [14]. Attempts to improve the situation in ChPT would imply the evaluation of higher order loop corrections and the corresponding counterterms. In general and for values of  $\mu \sim m_{\rho,\omega}$ , next order loop corrections in ChPT are found to be around 10-20% of the preceding order amplitude. We have confirmed this feature when going from the lowest order amplitude (4) to the one including one-loop effects. For these reasons we don't compute the (otherwise difficult) two-loop corrections which are expected to be smaller than others coming from uncertainties in our model and the values of its parameters.

By contrast, corrections coming from counterterms have been shown to be larger and the evaluation of higher-order ones under our assumption of resonance saturation is trivial. As in ref.[11], the introduction of the whole vector-meson form-factor  $m_{\rho,\omega}^2/(m_{\rho,\omega}^2 - s)$  (instead of its truncated series  $1 + s/m_{\rho,\omega}^2$ ) represents an "all-order" estimate of our resonance dominated counterterms. Taking into account the physical finite widths [8] of the  $\rho$  and  $\omega$  mesons, this amounts to write

$$\sigma_{e^+e^- \rightarrow \rho,\omega \rightarrow \pi^0\gamma}(s) = \frac{\alpha^3}{12\pi^2 f^2} (1 - m_{\pi^0}^2/s)^3 \left| C_l(\mu = m_{\rho,\omega}, s) + \frac{1}{2}P_\rho(s) + \frac{1}{2}P_\omega(s) \right|^2$$

$$P_V(s) \equiv m_V^2/(m_V^2 - s - i\sqrt{s}\Gamma_V), \quad V = \rho^0, \omega \quad (20)$$

The corresponding prediction is also shown (solid line) in Fig.1. The agreement at the  $\omega$ -peak (158 nb vs  $152 \pm 13$  nb from experiment [14]) is essentially a consequence of having used  $a_2 + 2a_3 = -3/8\pi^2$ , and  $\Gamma_{\omega \rightarrow all} = 8.43 \pm 0.10$  MeV and  $BR(\omega \rightarrow \pi^0\gamma) = (8.5 \pm 0.5)\%$  [8], quite close to  $8.4 \pm 0.1$  MeV and  $(8.88 \pm 0.62)\%$  as measured in [14] from the  $e^+e^- \rightarrow \omega \rightarrow \pi^0\gamma$  cross-section at the  $\omega$  peak.

Turning to the  $e^+e^- \rightarrow \pi^0\gamma^*$  transition, i.e., allowing for the final state photon to

be also off-mass-shell ( $k^{*2} > 0$ ) as in  $e^+e^- \rightarrow \pi^0 l^+ l^-$ , leads to

$$\sigma_{e^+e^- \rightarrow \rho, \omega \rightarrow \pi^0 \gamma^*}(s, k^{*2}) = \frac{\alpha^3}{12\pi^2 f^2} \left(1 - \frac{(m_\pi + \sqrt{k^{*2}})^2}{s}\right)^{3/2} \left(1 - \frac{(m_\pi - \sqrt{k^{*2}})^2}{s}\right)^{3/2} \cdot \left[ \left(1 + \frac{2a_2}{a_2 + 2a_3} \frac{k^{*2}}{m_{\rho, \omega}^2 - k^{*2}}\right) \frac{P_\rho(s) + P_\omega(s)}{2} + \left(1 - \frac{2a_2}{a_2 + 2a_3}\right) \frac{k^{*2}}{m_{\rho, \omega}^2 - k^{*2}} + C_l(\mu, s) + C_l(\mu, k^{*2}) \right] \quad (21)$$

where only one-loop effects have been included for both virtual photons in the last terms, whereas an ‘‘all-order’’ correction in the sense of the preceding paragraph is given for both  $s$ - and  $k^{*2}$ -dependent counterterms. Since in the latter case one always has  $k^{*2} < m_{\rho, \omega}^2$  we have introduced an averaged and simplified form-factor  $P_\rho(k^{*2}) \simeq P_\omega(k^{*2}) = 1 + k^{*2}/(m_{\rho, \omega}^2 - k^{*2})$ .

Eq.(21) has been plotted in Fig.2 for different values of the final virtual photon mass and the parameters  $a_2$  and  $a_3$  with the constraint  $a_2 + 2a_3 = -3/8\pi^2$ . The dashed line corresponds to the choice  $a_2 = 6a_3$ , eq.(18), and is considerably higher than the VMD choice  $a_2 = 2a_3$ , eq.(17), also shown as a solid line. For comparison, we also plot the (dotted) curve corresponding to  $a_2 = 0$ ,  $2a_3 = -3/8\pi^2$  which implies even smaller cross-sections and suggests that an experimental discrimination among the different values of  $a_2/a_3$  is indeed feasible. From the experimental point of view the prediction for the total  $e^+e^- \rightarrow \pi^0 \mu^+ \mu^-$  cross-section is more interesting. This has been plotted in Fig.3 again for  $a_2 = 6a_3$ ,  $2a_3$  and 0 (dashed, solid and dotted lines) and implies an  $\omega$ -peak cross-section  $\sigma_{e^+e^- \rightarrow \pi^0 \mu^+ \mu^-}(s = m_\omega^2) = 0.180$ , 0.145 and 0.089 nb, respectively. The corresponding experimental value  $0.164 \pm 0.040$  nb [12, 14] favours the first two possibilities but, again, new experiments could contribute to clarify the situation. This is not the case for the  $e^+e^- \rightarrow \pi^0 e^+ e^-$  cross-section (also shown in Fig.3) where the predictions for different values of  $a_2/a_3$  are quite similar due to the dominance of small  $k^{*2}$  values which reduces the sensitivity on  $a_2/a_3$  as seen in eq.(21).

In summary,  $e^+e^- \rightarrow \pi^0 \gamma$  and  $e^+e^- \rightarrow \pi^0 \mu^+ \mu^-$  cross-sections at low energy seem particularly interesting to test ChPT. A definite, next-to-leading order prediction is given for the first reaction. The second one is shown to be more relevant when studying the saturation of the counterterms by resonances, which in this case are expected to be the well-known and non-strange  $\rho^0$  and  $\omega$  vector-mesons. Their incorporation in the theory along the lines of Bando et al. [10], eqs.(13) and (14), or similar approaches can be greatly clarified, as well as the connection of these schemes with the conventional VMD model. The possible violation of this model observed in  $\omega \rightarrow \pi^0 \mu^+ \mu^-$  decays [12] can be simply accommodated in our present, wider context. Similar effects could be detected and studied in  $\pi^0$  production experiments with two (considerably) virtual photons,  $e^+e^- \rightarrow e^+e^- \gamma^* \gamma^* \rightarrow e^+e^- \pi^0$ [15]. In both cases, low energy  $e^+e^-$  machines or  $\phi$ -factories could provide valuable data.

### Acknowledgements

A.B. thanks the Frascati Theory Group for their kind hospitality and CICYT for partial financial support. Discussions with J.Bijnens, E.Pallante and R.Petronzio are also acknowledged.

### References

- [1] L. Maiani, "Theory Working Group: Summary of the results" in Proceedings of the Workshop on Physics & Detectors at DAPHNE, Frascati 9-11 Aprile 1991, Ed. by G.Pancheri, INFN-Laboratori Nazionali di Frascati. Frascati (1991).  
"Proposal for a  $\Phi$ -factory", LNF-90/031(R), Laboratori Nazionali di Frascati-INFN, 30 Aprile 1990.
- [2] J. Gasser and H. Leutwyler, Ann. Phys. 158 (1984) 142  
J. Gasser and H. Leutwyler, Nucl. Phys. B250 (1985) 465, 517.
- [3] G. Ecker et al., Nucl. Phys. B321 (1989) 311  
G. Ecker et al., Phys. Lett. B223 (1989) 425.
- [4] J.F. Donoghue, C. Ramirez and G. Valencia, Phys. Rev. D39 (1989) 1947.
- [5] J. Wess and B. Zumino, Phys. Lett. B37 (1971) 95.  
E. Witten, Nucl. Phys. B223 (1983) 422.
- [6] J.F. Donoghue, B.R. Holstein and Y.-C.R. Lin, Phys. Rev. Lett. 55 (1985) 2766.  
J. Bijnens, A. Bramon and F. Cornet, Phys. Rev. Lett. 61 (1988) 1453.  
J. Bijnens, A. Bramon and F. Cornet, Phys. Lett. 237B (1990) 488.
- [7] J. Bijnens, A. Bramon and F. Cornet, Z Phys. C46 (1990) 599.
- [8] Particle Data Group, Phys. Lett. 239B (1990) 1
- [9] CELLO Collaboration, Z Phys. C49 (1991) 401.
- [10] M. Bando, T. Kugo and K. Yamawaki, Phys. Rep. 164 (1988) 217.  
T. Fujiwara et al., Progr. Theor. Phys. 73 (1985) 926.
- [11] A. Bramon, E. Pallante and R. Petronzio, Phys. Lett. B, *in press*.
- [12] R.I. Dzhelyadin et al., Phys. Lett. 102B (1981) 296.
- [13] M. Crisafulli and V. Lubicz, in "Report on Physics at DAPHNE" Ed. by L. Maiani (in preparation).
- [14] S.I. Dolinsky et al., Phys. Rep. 202 (1991) 99.
- [15] E. Pallante and R. Petronzio, work in progress.



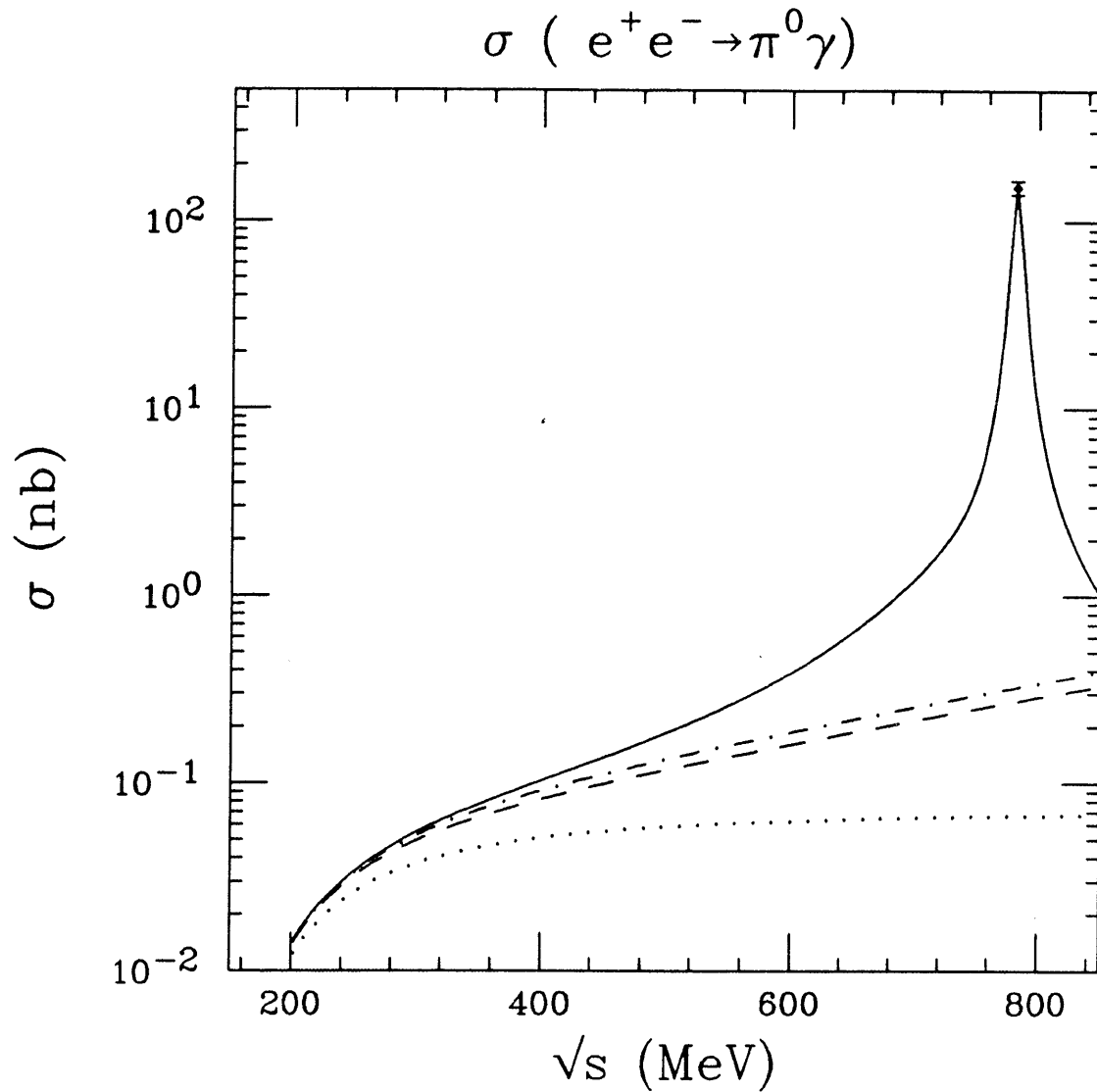


**Fig.1** Cross-section for  $e^+e^- \rightarrow \pi^0\gamma$  as a function of the total CM energy,  $\sqrt{s}$ . Dotted line corresponds to the lowest order result. Dashed line includes the counterterm contribution at the next order. Dot-dashed line represents the full ChPT prediction (with loop and counterterm corrections) at next-to leading order. Full line is the “all-order” result (see text).

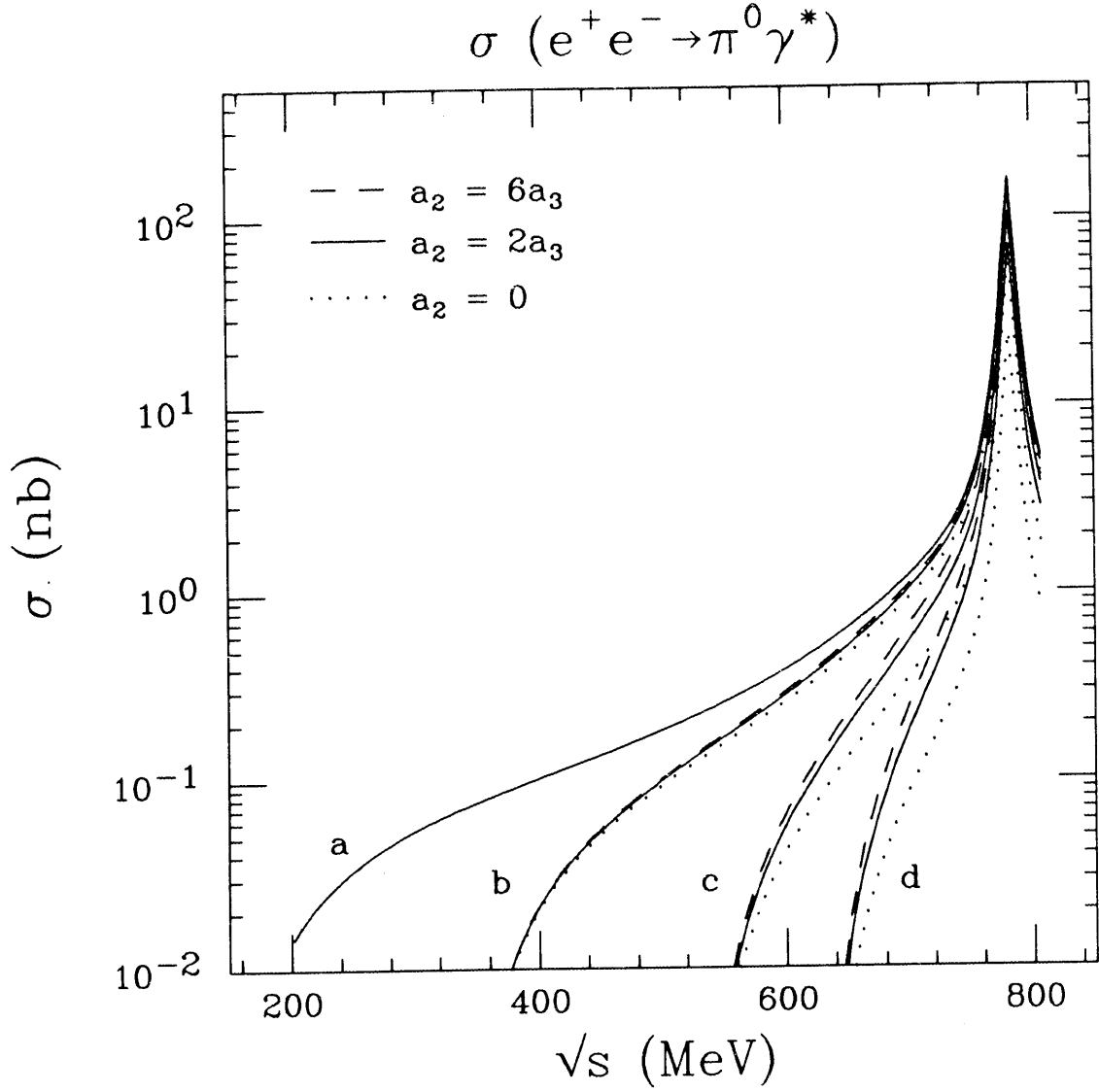


**Fig.2** Cross-section for  $e^+e^- \rightarrow \pi^0 \gamma^*$ , for different values of the final virtual photon mass and for different choices of the  $a_2, a_3$  parameters, with the constraint  $a_2 + 2a_3 = -3/8\pi^2$ . Curves labeled *a, b, c, d*, are for  $k^{*2} = 0, 4m_\mu^2, 0.16$  and  $0.25 \text{ GeV}^2$ , respectively.

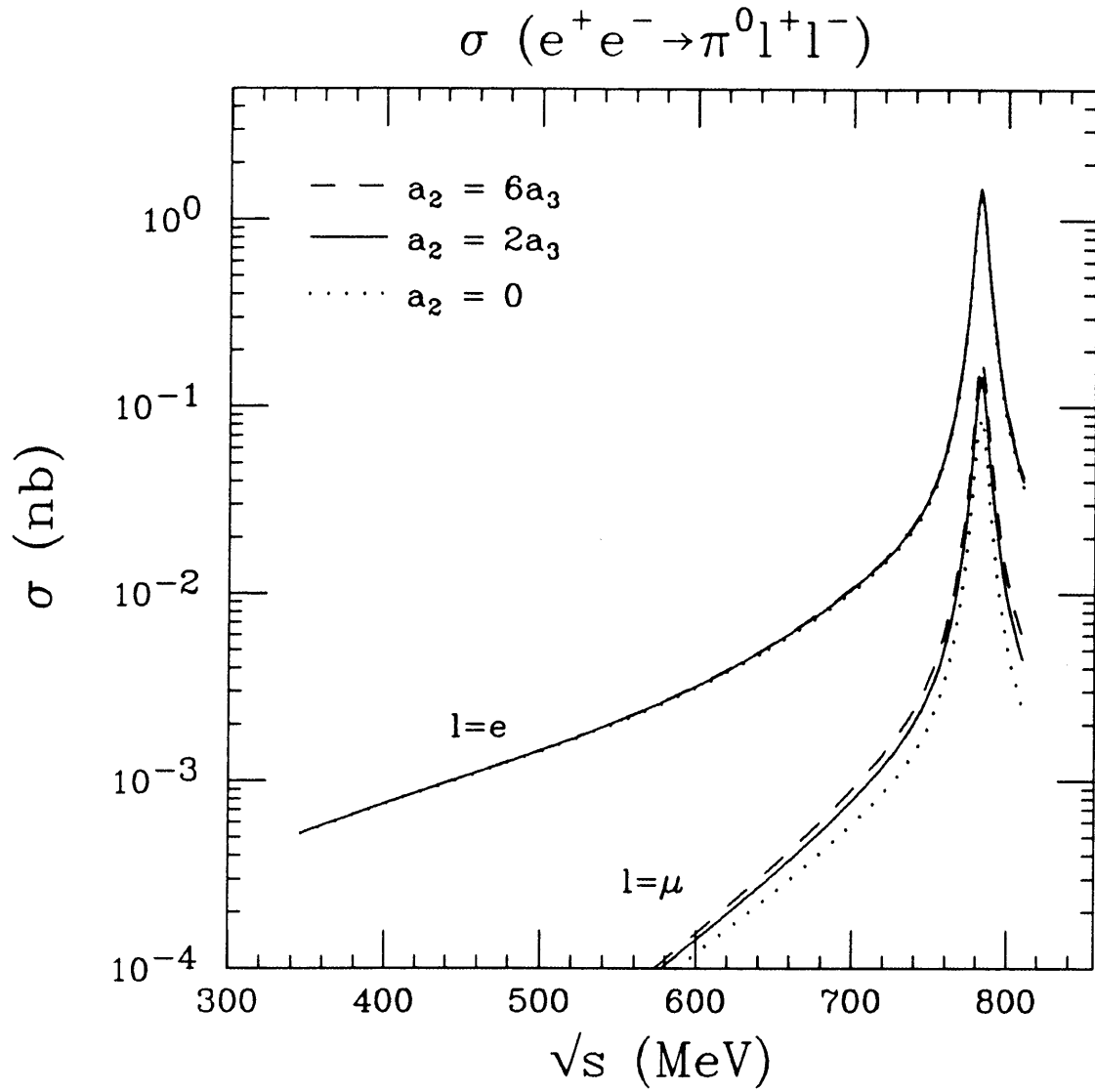


**Fig.3** Cross-section for  $e^+e^- \rightarrow \pi^0 \mu^+ \mu^-$  and  $\pi^0 e^+ e^-$  for the same values of the  $a_2$ ,  $a_3$  parameters as in Fig.2